A Study of 2*H*- and 2*D*-Benzotriazole in Their Lowest Electronic States by UV−Laser Double-Resonance Spectroscopy

Wolfgang Roth, Christoph Jacoby, Arnim Westphal, and Michael Schmitt*

Institut für Physikalische Chemie und Elektrochemie I, Heinrich-Heine-Universität Düsseldorf, D-40225 Düsseldorf, Germany

Received: November 18, 1997; In Final Form: February 18, 1998

Hole-burning spectra of 2*H*-benzotriazole and 2*D*-benzotriazole have been recorded in a range 1250 cm^{-1} above the electronic origin to rule out the possibility that the other tautomer (1*H*-benzotriazole) absorbs in this frequency range. After establishing the existence of only one absorbing species by spectral hole-burning spectroscopy, dispersed fluorescence spectra taken through several low-frequency vibronic bands of 2*H*(2*D*)-benzotriazole have been recorded. The ground-state vibrational frequencies are compared to results of an ab initio MP2 based normal-mode analysis. Assignments of S_1 vibrations to specific ground-state vibrations were established using the propensity rule. The rotational band contours of the vibronic 2*H*- and 2*D*-benzotriazole transitions have been determined to be pure *a*- or *b*-type. This can be traced back to the existence of two close lying electronically excited states of 2*H*-benzotriazole.

I. Introduction

Benzotriazole (BT) and its derivatives have found considerable interest due to their tautomeric equilibrium between the 1*H*- and the 2*H*-tautomer (Figure 1). This intramolecular proton-transfer enables BT to act as UV stabilizer and photographic restrainer. BT is also a very effective corrosion inhibitor for copper and its alloys, which was shown to be due to chelation of Cu via the nitrogen atoms 1 and 3 of BT.[1] Furthermore, derivatives of BT are used as antibacterial agents.

The exclusive presence of 1*H*-BT in the gas phase at high temperatures has been concluded by Maquestiau et al.[2] using electron impact fragmentation of BT and its *N*-methylated derivatives. However, it could be shown in a UV experimental study by Catalán et al.[3] that at lower temperatures the amount of the 2*H*-tautomer increases. Thus, the 2*H*-tautomer is more stable and predominant in the gas phase at lower temperatures.

The crystal structure of BT was determined by Escande et al.[4] via X-ray diffraction. All molecules in the unit cell belong to the same configuration, which could be proven to be the 1*H*-tautomer. This was further confirmed by experimental and theoretical studies of the ^{14}N quadrupole tensors in crystalline BT.[5]

Structure and dipole moment components of 1*H*-benzotriazole have been obtained by microwave spectroscopy in a heated cell[6] as well as in a molecular beam.[7] The molecule is planar in its electronic ground state; the dipole moment components were determined to be $\mu_a = 2.9$ D and $\mu_b = 3.2$ D. The 2*H*-tautomer could not be observed in the gas phase via microwave spectroscopy probably due to a 6−10 times smaller dipole moment of the C_{2v}-symmetric 2*H*-BT.

Structure and relative stabilities of both conformers have been subject to a plethora of theoretical studies on very different levels of theory. The order of stabilities depends crucially on the extent of electron correlation included in the calculations and consideration of zero-point energies (ZPEs). Molecular mechanics (PM3, AM1), semiempirical (MNDO),[8] and HF−SCF calculations with the 6-31G basis set[9] favor the 1*H*-tautomer. Even a fully optimized HF/6-31G(d,p) calculation including ZPE shows the 1*H*-tautomer to be more stable. Nevertheless, Thomás et al. showed that a full optimization at the MP2/6-31G(d,p) level reverses the relative stabilities of 1*H*- and 2*H*-BT.[10] They proposed that lone pair repulsion predominates aromaticity, thus favoring the 2*H*-tautomer. Relative stabilities of the two tautomers have also been obtained using the BLYP functional with the 6-31G(d) basis by Negri and Caminati[11] and with the B3LYP functional with the same basis by Fischer et al.[12] Using density function theory (DFT) methods, the energy difference decreases compared to the HF or MP2 calculations. In fact, the difference becomes so small that consideration of ZPE reverses the order again, favoring the 1*H*-tautomer.[13] Vertical excitation energies, oscillator strengths, and transition dipole moments for the lowest electronically excited state of both isomers have been computed with the CIS method.[11]

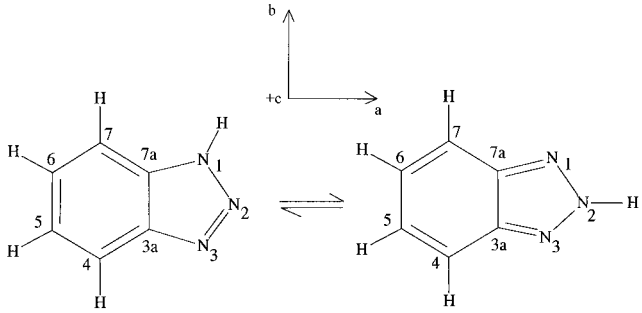

Figure 1. Tautomeric equilibrium between 1*H*- and 2*H*-benzotriazole and their atomic numbering. The inset shows the inertial axes of 2*H*-BT. The *a*- and *b*-axes of 1*H*-BT are rotated around the *c*-axis only by 0.5° regarding the same molecular orientation as in 2*H*-BT.

The vibrational spectrum of 2*H*-BT has been calculated by Fischer et al.[12] by analytical second differentiation with respect to the nuclear displacements based on the fully optimized MP2/6-31G(d) geometries.

The vibrational structures of BT and several derivatives have been studied in the gas phase using IR,[14] FTIR,[12,15] and Raman

* To whom correspondence should be sent.

S1089-5639(98)00239-4 CCC: $15.00
Published on Web 04/30/1998

spectroscopy[15] as well as in KBr pellets[16] and in single crystals using polarized IR and Raman spectroscopy.[17] The assignment of vibrational transitions to normal modes of BT has been aided by FTIR spectroscopy of the N-deuterated isotopomer in a supersonic jet. Under the reported experimental conditions less than 10% of the less stable 1*H*-tautomer is present in the jet.[12]

Polarized absorption and fluorescence measurements in different solvents revealed the existence of three electronically excited singlet states[18] which are labeled as ^1L_a, ^1L_b, and ^1B_b, following the nomenclature of Platt.[19] Measurements in polar and apolar aprotic solvents show that in solution BT exists predominantly in the 1*H*-tautomeric form.[20] The existence of several (close lying) electronic states *and* two different conformers, possibly absorbing in the same spectral region, further complicates the interpretation of the electronic spectra.

Gas-phase UV spectra of BT and its *N*-methyl derivatives have been reported by Catálan et al.[3] From thermodynamical considerations they determined the relative stabilization of the 2*H*-tautomer to 3.8 kcal mol^{-1}. Jalviste et al.[21] measured the LIF and dispersed fluorescence spectrum of BT in a supersonic jet. From the Franck−Condon pattern of the emission spectrum they presumed a large geometry change upon electronic excitation. The excitation spectrum terminates rapidly above 1200 cm^{-1}, which is due to an effective coupling to a nonradiative manifold. The rotational band contour of the 286 nm band system of BT has been measured by Cané et al.[22] A simulation of their spectrum yielded rotational constants that were believed to belong to the 1*H*-tautomer. This was disproved by Berden et al.,[23] who obtained accurate rotational constants from a rotationally resolved UV spectrum of the $\pi^* \leftarrow \pi$ transition at 34 917.8 cm^{-1} in a supersonic jet. They found that the electronic spectrum of BT is due to absorption of the 2*H*-tautomer ($^1B_2 \leftarrow {}^1A_1$) and determined the radiative lifetime of BT to 1.1 ns.

The vibronic spectrum of the C_{2v}-symmetric 2*H*-BT exhibits more bands than can be explained by normal modes, their (harmonic) overtones, and combination bands.[21] The aim of this work is to study the vibrations of BT in its ground and first electronically excited states experimentally using dispersed fluorescence (DF), laser induced fluorescence (LIF), one- and two-color resonant two-photon ionization (R2PI), and spectral hole burning (SHB).

Depending on the relative energy of the two isomers, both species can be present under the experimental conditions. Dispersion of single vibronic level fluorescence (SVLF) of vibronic states, which are shown to belong to the 2*H*-tautomer, should yield ground-state vibrational levels of the same isomer. However, this assumption is valid only if proton transfer between the two isomers is unfeasible during electronic excitation and fluorescence. Thus the DF spectra should be free of disturbances from the 1*H*-species. This may not be the case for direct observations via IR/FTIR or Raman spectroscopy.

A vibrational assignment of ground and electronically excited states will be presented, based on the results of ab initio Møller−Plesset perturbation theory to second order (MP2).

II. Experimental Section

The R2PI measurements were carried out using the frequency-doubled output of a Nd:YAG (Spectra Physics, GCR170) pumped dye laser (LAS, LDL205) operated with Fluorescein 27. For hole-burning spectroscopy the second harmonic of a Nd:YAG (Spectra Physics GCR3) pumped dye laser (LAS, LDL205) was used, operated with Fluorescein 27 dye.

The second harmonic of this laser counterpropagates the first one in the ionization chamber. To improve the hole-burning signal, the fundamental of the hole-burning laser was used together with the second harmonic. Both lasers have been calibrated by comparison with an iodine spectrum.[24]

The apparatus used for spectral hole burning and R2PI consists of a source chamber pumped with a 1000 L/s oil diffusion pump (Alcatel) in which the molecular beam is formed by expanding a mixture of helium and benzotriazole through the 300 μm orifice of a pulsed nozzle (General Valve, Iota One). Dried benzotriazole was heated to 150 °C prior to expansion. The skimmed molecular beam (Beam Dynamics Skimmer, 1 mm orifice) crosses the laser beams at right angles in the ionization chamber. The ions are extracted in a gridless Wiley−McLaren type time-of-flight (TOF) spectrometer (Bergmann Messgeräte Entwicklung) perpendicular to the molecular beam and laser direction and enter the third (drift) chamber, where they are detected using multichannel plates (Galileo). Ionization and drift chamber are both pumped with a 150 L/s rotatory pump (Leybold). The vacuum in the three chambers with the molecular beam on was 1×10^{-3} mbar (source), 5×10^{-5} mbar (ionization), and 1×10^{-7} mbar (drift), respectively.

The resulting TOF signal was digitized by a 500 MHz oscilloscope (TDS 520A, Tektronix) and transferred to a computer, where the TOF spectrum was recorded by means of a program, written in LabVIEW (National Instruments). This program allowed us to record as many mass traces as necessary, to control the scanning of the laser and to display, save, and plot the spectrum.

The Q-switch of the laser(s) and the TOF voltage ramp were triggered by a digital delay generator (Stanford DG535) together with a home-built delay generator for the triggering of laser flashlamps and pulsed nozzle. Timing stability was better than 2 ns.

The fluorescence emission spectra were taken in a vacuum chamber pumped with a 2000 L/s oil diffusion pump (Edwards). The second harmonic of an excimer (EMG 200 E, Lambda Physik, operated at 308 nm) pumped dye laser (FL 3002, Lambda Physik, operated with Coumarin 153) was used for excitation. The emitted fluorescence was collected and focused by a two-lens system on the entrance slit of a 1 m Czerny−Turner monochromator with an aperture of *f*/8.4 (Jobin Yvon THR 1000). We used a holographic grating (11 cm × 11 cm) with 2400 grooves/mm blazed to 280 nm in second grating order. The resulting linear dispersion dλ/dx at 280 nm is 3.6 Å/mm. The fluorescence is imaged on the photocathode of the CCD camera, intensified, and recorded on the CCD chip after 15:25 reduction of the image size in an optical fiber taper. With a CCD chip width of 1/3 in. and a pixel size of 23 μm × 23 μm, a range of ≈650 cm^{-1} of the emission spectrum can be taken in one grating position of the monochromator in first order.

The dispersed fluorescence is recorded with 12 bit resolution by the intensified slow scan gated CCD camera (LaVision, Flame Star) positioned in the image plane of the monochromator. The resulting two-dimensional array (x = height of the entrance slit; y = dispersion) is averaged over a curved x-range, to compensate for errors due to the spherical aberration of the mirrors.

A single fluorescence excitation spectrum was obtained by summing the fluorescence of 200 laser pulses on the CCD chip and subtracting the background straylight (gas pulse off) after 200 laser pulses. Depending on the intensity 30−200 of these spectra had to be averaged to obtain the displayed spectra.

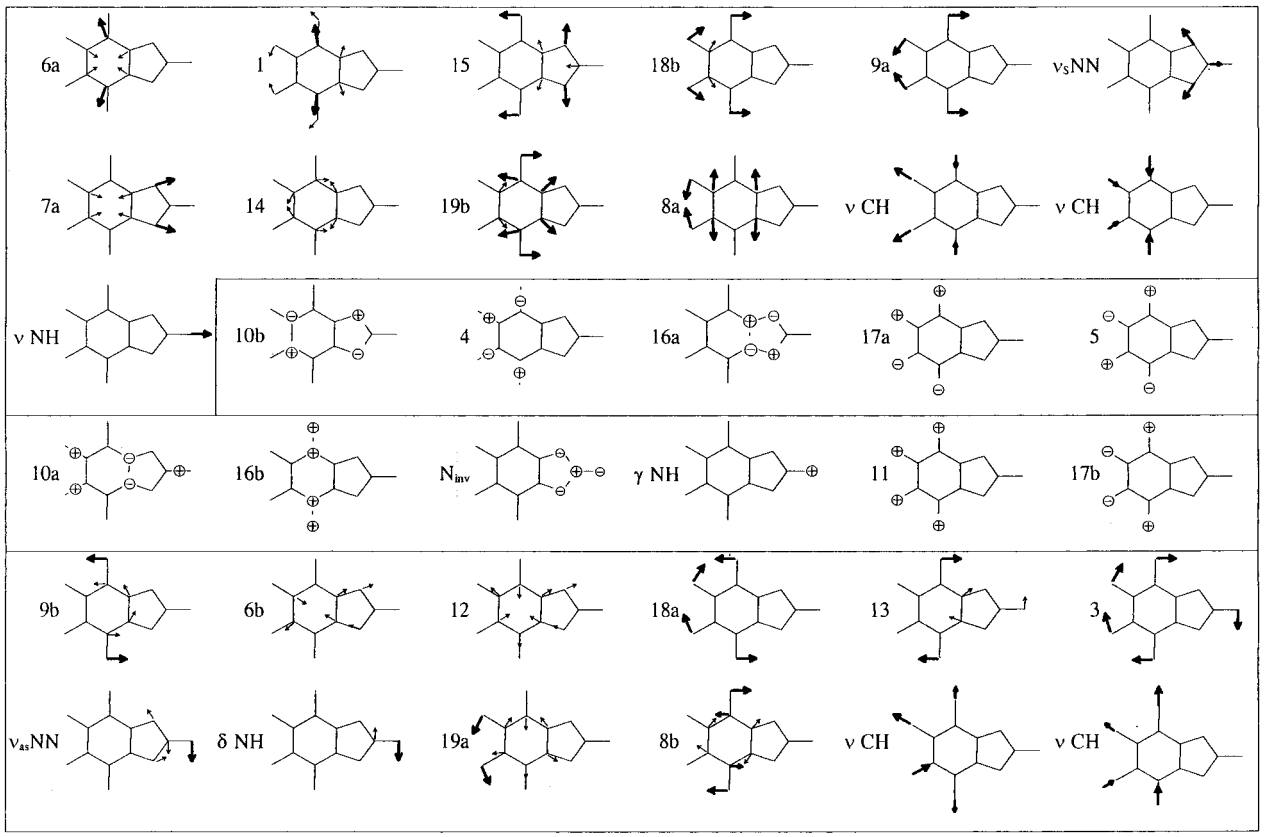

Figure 2. Atomic displacement vectors for the vibrational modes of 2*H*-benzotriazole. The nomenclature is adopted from Varsanyi[26] for ortho-di-light-substituted benzene derivatives and completed for vibrations of the five-membered ring. The vibrations are sorted by their symmetries (a_1, a_2, b_1, b_2) and by ascending frequencies.

III. Theoretical Results

All ab initio calculations were performed using the Gaussian 94 program package.[25] The SCF energy convergence criterion was 10^{-8} hartree and the convergence criterion for the gradient optimization of the molecular geometry was 15×10^{-6} hartree/bohr and hartree/degree, respectively.

The ground state has been calculated by Møller−Plesset perturbation theory at second order (MP2) using the 6-311G-(d,p) basis set.

Due to the relatively high (C_{2v}) symmetry of 2*H*-BT, the calculated normal modes could be directly compared to the benzene vibrational modes presented by Varsanyi.[26] The displacement of atoms can be compared to the "ortho-di-light" substituted molecules, where the two nitrogen atoms are regarded as the ortho substituents. Therefore we will present our vibrational assignment in benzene-like nomenclature. However, it should be mentioned that the coupling of motions of the remaining N−H fragment to these normal modes depends strongly on the chosen method and basis set.

Figure 2 schematically shows the atomic displacements for all vibrational modes of 2*H*-benzotriazole. Bold arrows represent larger atomic displacements.

The usual description of normal modes in a molecule of this size by displacement vectors is difficult and even somewhat misleading (see below). In the past few years several programs became available, which visualize the normal vibrations by animated graphs. Most of these programs can directly read in the files of the Gaussian program. For the interested reader we made the .log files for the vibrations of 2*H*-BT available on our home page (http://www-public.rz.uni-duesseldorf.de/~pc1).

Table 1 gives the unscaled MP2 frequencies for 2*H*- and 2*D*-BT, the experimental frequencies from the DF measurements described in section IV.D, symmetries, and descriptions of the vibrational modes of 2*H*-BT. A problem of designation arises for the 2*H*-BT vibrations at 713 and 604 cm^{-1}. These vibrations can be described as pure out-of-plane bending motion γ NH of the hydrogen atom and an ammonia-like inversion vibration N_{inv}. For 2*D*-BT the vibration at 501 cm^{-1} can still be described as γ ND, but shows a small admixture of N_{inv} character in contrast to the undeuterated species. Due to this coupling the inversion N_{inv} of the deuterated species is strongly affected and can better be described as a γ NNN out-of-plane motion, cf. Table 1.

The geometry of 2*H*-benzotriazole has been constrained to C_{2v} symmetry during optimization. From high-resolution UV measurements[23] the S_1 state (^1L_a) is known to have (electronically) B_2 symmetry. Therefore vibronic transitions into this state with a_1, a_2, and b_2 vibrational symmetries are allowed with polarizations along the molecular *b*-, *c*-, and *a*-axes, respectively. The pure electronic transition has no dipole moment components along the *a*- and *c*-axes, so that the most intense vibrational bands are expected to be of a_1 symmetry with *b*-type rotational contours.

Application of the symmetry operations to the nuclear coordinates and the translational and rotational motions, respectively, leads to the representations

$$\Gamma_{nuc} = 14\,a_1 + 6\,a_2 + 8\,b_1 + 14\,b_2$$

$$\Gamma_{trans} = a_1 + b_1 + b_2$$

$$\Gamma_{rot} = a_2 + b_1 + b_2$$

which lead to the symmetries of the 36 vibrational modes:

$$\Gamma_{vib} = 13\,a_1 + 5\,a_2 + 6\,b_1 + 12\,b_2$$

TABLE 1: Comparison of the Calculated MP2/6-311G(d,p) and Experimental Vibrational Frequencies for 2*H*- and 2*D*-BT

mode description	2*H*-benzotriazole			2*D*-benzotriazole			symmetry
	calc	obs	obs/calc	calc	obs	obs/calc	
ν_s NH	3649	3486	0.96	2684	2598	0.97	a_1
ν_s CH	3239	*a*		3239	*a*		
ν_s CH	3220	*a*		3220	*a*		
8a	1611	1537	0.95	1610	1534	0.95	
19b	1497	1407	0.94	1496	1404	0.94	
14	1434	1375	0.96	1432	1374	0.96	
7a	1351	1316	0.97	1351	1309	0.97	
ν_s NN	1204	1154	0.96	1185	1148	0.97	
9a	1166	1124	0.96	1161	1124	0.99	
18b	1022	1000	0.98	1022	999	0.98	
15	978	971	0.99	974	966	0.99	
1	792	778	0.98	789	777	0.98	
6a	544	542	1.00	542	538	0.99	
ν_{as} CH	3235	*a*		3235	*a*		b_2
ν_{as} CH	3208	*a*		3208	*a*		
8b	1670	1569	0.94	1670	1568	0.94	
19a	1527	1449	0.95	1526	1446	0.95	
δ NH	1502	1414	0.94	1347	1296	0.96	
ν_{as} NN	1382	1304	0.94	1437	1390	0.97	
3	1306	1250	0.96	1275	1248	0.98	
13	1233	1189	0.96	1008	981	0.97	
18a	1138	1133	1.00	1144	1138	0.99	
12	897	866	0.97	875	860	0.98	
6b	631	626	0.99	631	624	0.99	
9b	415	417	1.00	409	409	1.00	
17b	901	1854[b]	1.03[c]	901	1854[b]	1.03[c]	b_1
11	741			738			
γ NH	713			501	924	0.98[c]	
N_{inv}	604	1239[b]	1.02				
γ NNN[d]				639			
16b	408	432[e]	1.05[c]	408	429[e]	1.05[c]	
10a	216	430[b]	1.00[c]	211			
5	900			900			a_2
17a	824			824			
16a	641			641			
4	444			444			
10b	253	526[b]	1.03[c]	253	526[b]	1.03[c]	

[a] In this spectral region too many bands show up to give an unambiguous assignment. [b] First (allowed) overtone. [c] Observed/calculated for the calculated harmonic overtone. [d] Compare with text. [e] Harmonic value calculated from $10b^2$ and 10b + 16b.

The normal modes in Figure 2 are sorted by their symmetries. The a_1 and b_2 modes represent motions that lie within the molecular plane.

IV. Experimental Results

A. LIF, R2PI, and Hole-Burning Spectra of 2*H*-Benzotriazole. The results from spectral hole burning are important to ensure that all bands observed in the LIF and R2PI spectra belong to only one ground state conformer. Berden et al.[23] showed by rotationally resolved LIF spectroscopy that the electronic origin of BT at 34 917.8 cm^{-1} definitely belongs to the 2*H*-tautomer. We have taken the vibronic spectrum of benzotriazole by LIF (Figure 3a), R2PI (Figure 3b) and by SHB (Figure 3c) between the electronic origin (0,0) at 34 917.8 cm^{-1} and 0,0 + 1200 cm^{-1}.

The electronic origin of 2*H*-benzotriazole is not observed in the one-color R2PI spectrum, because in this range the energy difference $E(S_1) - E(S_0)$ is smaller than $E(D_0) - E(S_1)$. The inset in Figure 3b shows the origin, obtained by two-color R2PI, with an ionization wavelength of 266 nm (fourth harmonic of a Nd:YAG laser).

Hole-burning spectra have been taken by scanning the burn laser over the region of interest, while monitoring the ground-state population of a selected species by R2PI with a second, delayed laser. Each time hole burning and analysis laser share a common ground-state level the R2PI signal of the second laser decreases.

The electronic origin of BT is known to belong to the 2*H*-tautomer.[23] After we had established that the origin and the vibronic band at 480.7 cm^{-1} belong to the same species, we utilized this band for analysis. It should be mentioned that upon two-color hole burning with very intense 266 nm radiation as ionization wavelength the electronic origin could be observed with the same signal strength as upon one-color hole burning. This shows that the ionization step contributes little to the *irreversible* depopulation of the ground state. The SHB spectrum in Figure 3c shows that all bands observed in the LIF and R2PI spectra can be assigned to the 2*H*-tautomer.

The first vibronic band appears at 238.7 cm^{-1} in the two-color experiment. In the one-color R2PI spectrum the first transition is observed at 328.5 cm^{-1}. Thus the value for the IP, uncorrected for the repelling electric field, is determined to be 8.72 eV < IP < 8.74 eV. This differs considerably from 9.20 eV given in ref 8. For the deuterated isotopomer the IP is found to lie between 8.70 and 8.72 eV.

The LIF and R2PI intensities are different, as can be seen from Figure 3a,b. Both traces show a rapid termination of the excitation spectrum above 1200 cm^{-1}, while the hole-burning spectrum (Figure 3c) continues to higher frequencies. This can be explained by some fast nonradiative process in the excited state, proton transfer, predissoziation, or crossing of a nearby electronic state.

Table 2 lists the vibrational frequencies as obtained from the LIF, R2PI, and SHB spectra shown in Figure 3 together with the LIF intensities.

In search for absorptions of the 1*H*-tautomer, we scanned a range of 500 cm^{-1} to the red and 2500 cm^{-1} to the blue of the 2*H*-BT origin. There were no references to absorptions of the other tautomer, which may be due to the very different nature of both chromophores (cf. Figure 1). Another reason may be very small excitation or ionization cross sections of the second tautomer. We will continue this quest in the near future, guided by the results of calculations on the electronically excited states of both tautomers.

B. R2PI Spectra of 2*D*-Benzotriazole. To obtain an assignment of the vibrations of 2*H*-BT both in the ground and electronically excited state, the employment of the N-deuterated isotopomer proved to be helpful. Figure 4b shows the one- and two-color R2PI spectra of 2*D*-BT. For direct comparison the R2PI spectrum of 2*H*-BT is displayed in Figure 4a.

The electronic origin of 2*D*-BT is shifted 53.7 cm^{-1} to the blue of the 2*H*-BT origin. This is very much, compared to a value of 5 cm^{-1} for indole[27] and 6.8 cm^{-1} for benzimidazole.[28] Such a large deuteration shift points to a considerable frequency change upon electronic excitation for at least one vibration involving the N−H bond. As in the case of the undeuterated species, the signal vanishes above 1200 cm^{-1}. The relative intensities obtained from R2PI differ considerably for 2*H*- and 2*D*-BT. The experimental frequencies and intensities of the d_1-isotopomer are presented in Table 3.

The large intensity differences between the spectra of the deuterated and undeuterated molecule prevent a straightforward assignment of shifted bands. Nevertheless, the fact that the shifted bands must have the same rotational band contour (see section IV.C) helps to get an unambiguous assignment of 2*D*- to 2*H*-transitions for most of the vibronic bands.

C. Rotational Band Contours. After we excluded the second tautomer as responsible for the multitude of bands in

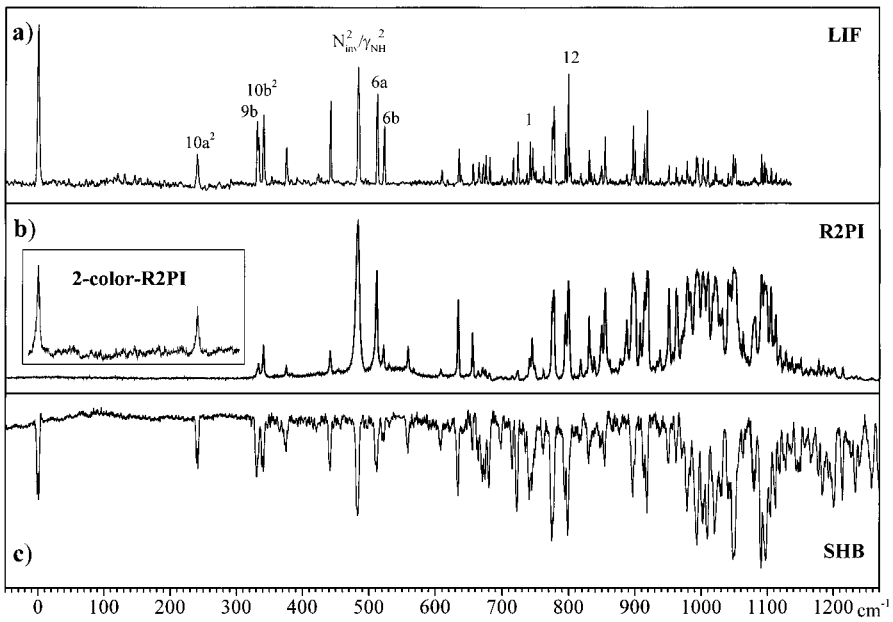

Figure 3. (a) LIF spectrum of 2*H*-BT between the electronic origin at 34 917.8 cm^{-1} and 0,0 + 1250 cm^{-1}. The width of the vibronic bands in the LIF spectrum is approximately 1.8 cm^{-1} and determined by a rotational temperature of 2.5 K. (b) R2PI spectrum in the same spectral region. The inset shows the electronic origin obtained by two-color R2PI, with an ionization wavelength of 266 nm. (c) Hole-burning spectrum, obtained via analysis of the band at 0,0 + 480.7 cm^{-1}.

TABLE 2: Vibrational Frequencies, LIF Intensities, and Rotational Band Contours of 2*H*-BT As Obtained from the LIF and R2PI Spectra

frequency[a]	intensity	band type	assignment	rel freq	intensity	band type	assignment
0	100	b	0,0	813.5	8	b	
238.7	22	b	$10a^2$	826.7	27	a	
328.5	43	a	9b	829.5	10	b	
330.7	31	b	$10b^2$	844.8	10	b	
338.2	47	b		850.3	35	b	
373.1	27	b		892.6	41	a	
439.2	59	a		895.9	27	a	
480.7	71	b	$N_{inv}^2/\gamma NH^2$	903.0	6	b	
481.9	63	a		909.6	22	a	
509.5	59	b	6a	914.1	51	a	
519.9	35	b		946.3	16	a	
631.9	22	a	6b	957.3	14	a	
653.1	14	a		973.7	18	b	
661.8	16	b	$10b^4$	987.4	18	b	
672.5	14	a		989.4	12	b	
678.2	22	a		997.4	18	b	
696.3	8	a		1005.5	18	a	
712.8	18	a		1016.5	12	a	
719.7	29	a		1035.8	8	a	
721.0	18	b		1038.9	6	a	
738.1	8	a		1043.5	22	a	
741.7	31	a		1045.7	18	a	
746.7	27	b		1086.7	20	a	
758.5	12	b		1090.6	14	a	
773.6	55	b		1094.3	12	a	
791.0	37	a		1096.5	12	a	
795.6	76	a		1108.2	8	b	
798.2	14	b		1116.1	4	a	

[a] Relative to the electronic origin at 34 917.8 cm^{-1}.

the BT spectrum, the question arises whether some of these bands may be due to excitation to another electronically excited state. A closer look at the fluorescence excitation spectra revealed that many of the bands possess band contours other than that of the electronic origin of 2*H*-BT, which has been determined to be pure *b*-type.[23] Figure 5 shows the rotational band contours of the vibronic bands at 439.2 cm^{-1} and the close pair at 480.7/481.9 cm^{-1}. This pair proved to be (accidentally) very close *a*- and *b*-type bands. The resolution of these spectra is 0.2 cm^{-1} due to our laser line width. The rotational temperature in the jet could be estimated to be 2.5 K. The *b*-type bands could be simulated with the rotational constants of ref 23 and a transition dipole moment in the direction of the inertial *b*-axis. All *a*-type bands were simulated using the same rotational constants together with pure *a*-type selection rules.

The last columns of Table 2 and Table 3 summarize the transition dipole moment orientations for all bands of the 2*H*- and 2*D*-BT which could be assigned.

The unexpectedly large number of *a*-type bands will be discussed in section V.B.

D. Dispersed Fluorescence Spectra of 2*H*- and 2*D*-Benzotriazole. To assign the computed vibrational frequencies to specific modes, we have measured dispersed fluorescence spectra after excitation of the most intense low-frequency vibronic levels of 2*H*-BT. In some of the spectra new bands appear, which are absent in the DF spectrum of the electronic origin. The spectra obtained via excitation of the electronic origins of 2*H*- and 2*D*-BT are displayed in Figure 6a,b between 0 and 3800 (3000 for 2*D*-BT) cm^{-1}. Due to selective excitation of this tautomer, the fluorescence will be uniquely from 2*H*-(2*D*-)BT, if no rearrangement to the other tautomer takes place in the S_1 state.

The observation of *all* vibrational modes demands the dispersion of fluorescence from more than one excited vibronic level. Otherwise, several bands may be missed due to unfavorable Franck−Condon factors. Additionally, spectra taken through different vibronic levels may help in the assignments of S_1 vibrations and in the examination of coupling between vibrational modes in the electronically excited state.

Figure 7a−j shows the SVLF spectra obtained by dispersing the fluorescence from several vibronic 2*H*-BT bands. Figure 8a−g displays the SVLF spectra obtained through some of the vibronic bands of 2*D*-BT. Table 4 and Table 5 summarize all experimental frequencies and intensities together with the assignments for 2*H*- and 2*D*-BT, respectively.

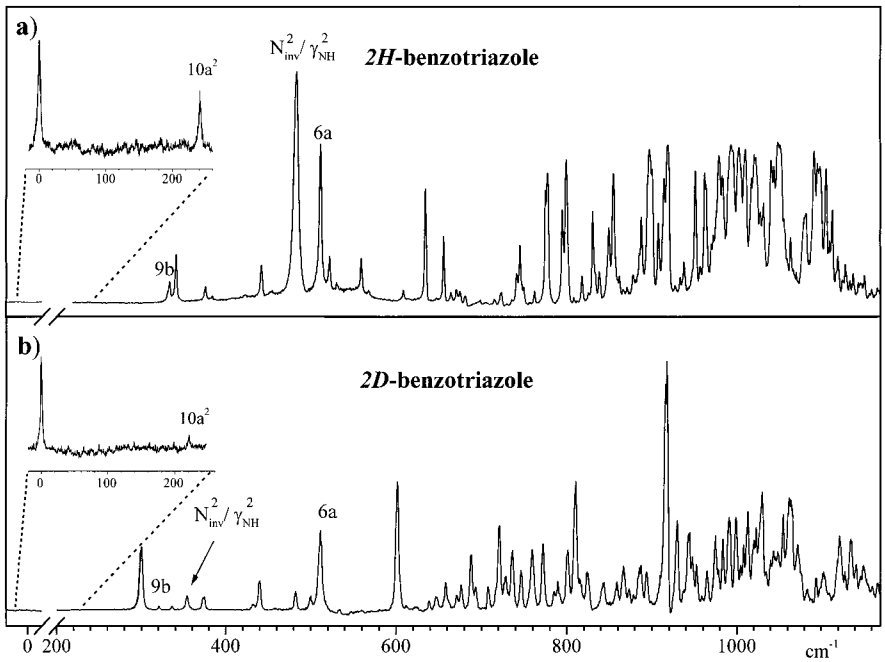

Figure 4. One-color R2PI spectrum of 2*D*-BT. The inset shows the two-color R2PI signal in the region of the electronic origin. The origin of the deuterated isotopomer is shifted by 53.7 cm^{-1} to the blue, compared to 2*H*-BT. The R2PI spectrum of 2*H*-BT is displayed in the upper trace for a direct comparison of frequency and intensity shifts.

TABLE 3: Experimental Frequencies, LIF Intensities, and Transition Dipole Moment Orientations of 2*D*-BT

frequency[a]	intensity	band type	assignment	rel freq	intensity	band type	assignment
0	100	b	0,0	769.4	30	a	
218.0	10	b	$10a^2$	786.9	10	b	
297.9	90	b		798.3	40	a	
319.0	40	a	9b	807.0	60	b	
335.8	20	b	$10b^2$	820.5	20	a	
352.3	50	b	$N^2_{inv}/\gamma NH^2$	823.1	10	b	
372.1	50	b		890.5	20	a	
438.4	60	a		912.9	100	a	
481.0	30	a		971.1	10	a	
498.6	20	b		980.3	10	a	
510.1	80	b	6a	987.6	20	b	
516.4	10	b		990.2	10	a	
599.6	20	a		995.4	30	b	
686.0	20	a		1004.4	10	a	
705.0	10	b		1009.2	20	b	
718.3	50	b		1019.1	10	b	
725.3	20	b		1058.5	30	a	
733.1	60	a		1061.6	20	b	
756.7	30	b					

[a] Relative to the electronic origin at 34 971.5 cm^{-1}.

V. Discussion

A. Electronic Ground State. In the following only the observed fundamental vibrations and overtones of forbidden bands will be discussed, while combination bands and overtones of allowed fundamentals are listed in Table 4 and Table 5.

The lowest frequency band in the DF spectra of 2*H*-(2*D*-)-BT is observed at 417 (409) cm^{-1}. It is assigned to a benzene-like 9b vibration with b_2 symmetry and appears strongly when pumping the bands at 328.5 and 439.2 cm^{-1} and with weaker intensity via the bands at 481.9 and 795.6 cm^{-1}. These S_1 vibronic bands are all *a*-type rotational transitions and may therefore be assigned to b_2 modes. The 9b mode at 417 cm^{-1} is the strongest band upon excitation at 328.5 cm^{-1}, which is therefore assigned to the 9b mode in the S_1 state, while 409 cm^{-1} for 2*D*-BT shows a very strong propensity for 319.0 cm^{-1} in the S_1 state. The deuteration shift of 2% in the S_0 state is in good agreement with the calculations. The experimental value of 2.7% for the S_1 state is close to that.

Because no further fundamentals are expected in this spectral region, the transition at 430 cm^{-1} has to be assigned to an overtone of a nontotally symmetric vibration. Comparison to the calculations points to the out-of-plane bending vibration 10a, which has a calculated fundamental frequency of 216 cm^{-1}. This vibration appears upon excitation of the 238.7 cm^{-1} band. Therefore we very tentatively assign the vibronic band at 238.7 cm^{-1} to $10a^2$ in the S_1 state. Another indication of the correctness of this assignment is the strong appearance of a band at 833 cm^{-1} upon excitation of the 238.7 cm^{-1} mode. We have assigned this band to a combination of the 10a vibration (b_1) with the fundamental of the N(2) inversion N_{inv} (b_1) resulting in an allowed a_1 band.

The band at 542 (538) cm^{-1} has to be assigned to the totally symmetric ring breathing vibration 6a, while 626 (625) cm^{-1} is assumed to be the 6b vibration. The totally symmetric 6a is mainly observed upon excitation of *b*-type modes. A distinct progression of the 6a mode dominates the spectrum obtained upon excitation at 509.5 cm^{-1}.

According to our calculations the following fundamentals are the totally symmetric benzene ring breathing mode 1 and the b_2 mode 12, which are found experimentally at 778 (777) cm^{-1} and 866 (860) cm^{-1}. They are both very weak and can be observed only upon excitation of the vibronic bands at 519.9 and 795.6 cm^{-1}, respectively. The totally symmetric vibrations 15 and 18b are present in almost every DF spectrum and are located at 971 (967) cm^{-1} and 1000 (999) cm^{-1}. The next a_1 fundamental is the 9a band at 1124 (1124) cm^{-1}.

The very intense band at 1154 (1148) cm^{-1} is assigned to a vibration that is mainly localized in the five-membered heterocyclic ring and can approximately be described as a symmetric N−N stretching vibration (ν_s NN).

The strongest band upon excitation of 0,0 is observed at 1239 cm^{-1}. Despite its intensity, we assign this band to the first overtone of the umbrella mode N_{inv}, which has b_1 symmetry. The third and fifth overtone of this out-of-plane motion are

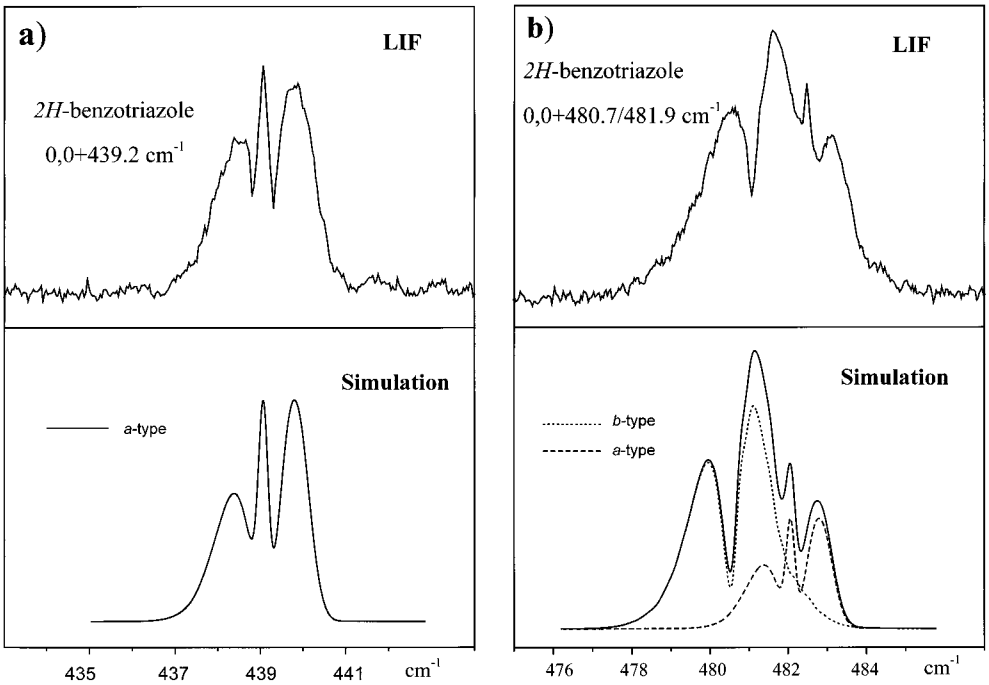

Figure 5. Experimental (upper trace) and simulated (lower trace) rotational band contours of three different vibronic bands of 2*H*-BT. (a) Rotational band contour of the vibronic band at 0,0 + 439.2 cm^{-1}. The rotational constants for the simulation have been taken from ref 23; the direction of the transition dipole moment is along the inertial *a*-axis. (b) Rotational band contour of the vibronic bands at 480.7/481.9 cm^{-1}. The 480.7 cm^{-1} band has been simulated assuming a pure *b*-type spectrum (dotted line), while the 481.9 cm^{-1} band was simulated as a *a*-type band (dashed line).

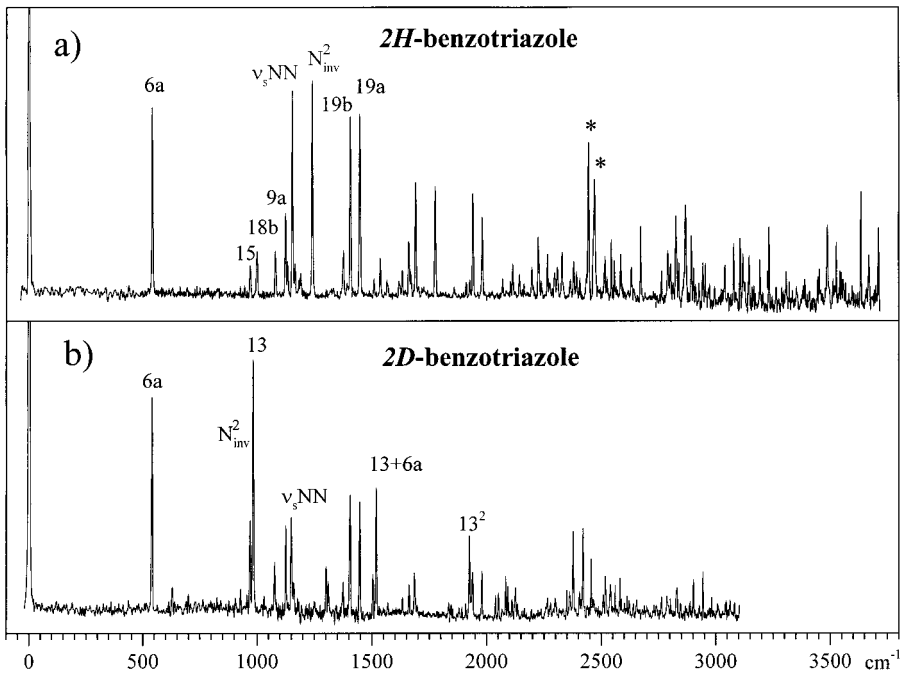

Figure 6. (a) SVLF spectrum of 2*H*-BT between 0 and 3800 cm^{-1} obtained via excitation of the electronic origin. Spectral resolution is ≈1.6 cm^{-1}. The bands marked with an asterisk are due to 308 nm excimer stray light. (b) SVLF spectrum of 2*D*-BT between 0 and 3000 cm^{-1} obtained upon excitation of 0_0^0.

observed at 2480 and 3724 cm^{-1}. An alternative assignment to the CH-bending mode 3 (cf. Table 1) does not seem very reasonable, because the other CH-bending vibrations (9a, 18a, and 18b) are quite weak and show little effect upon N-deuteration, while no nearby band shows up in the 2*D*-BT spectra.

The next a_1 fundamental is found at 1316 (1309) cm^{-1} and can be assigned to the mode 7a. A vibration with a distinct positive deuteration effect is the asymmetric stretching mode ν_{as} NN. The fact that the 1304 cm^{-1} band in the 2*H*-BT spectrum has no obvious unshifted counterpart in the deuterated spectrum leads to the assignment of this band to the asymmetric stretch. The shifted band can be found at 1390 cm^{-1} in fair agreement with the calculations.

The totally symmetric ring deformation vibrations 14 (1375 cm^{-1}) and 19b (1407 cm^{-1}) are observed close to the unscaled MP2/6-311G(d,p) frequencies and show the predicted small deuteration shifts of 1 and 3 cm^{-1}, respectively. The following fundamental at 1414 cm^{-1} shows a very large isotopic shift (−118 cm^{-1}) and can be described according to the calculations

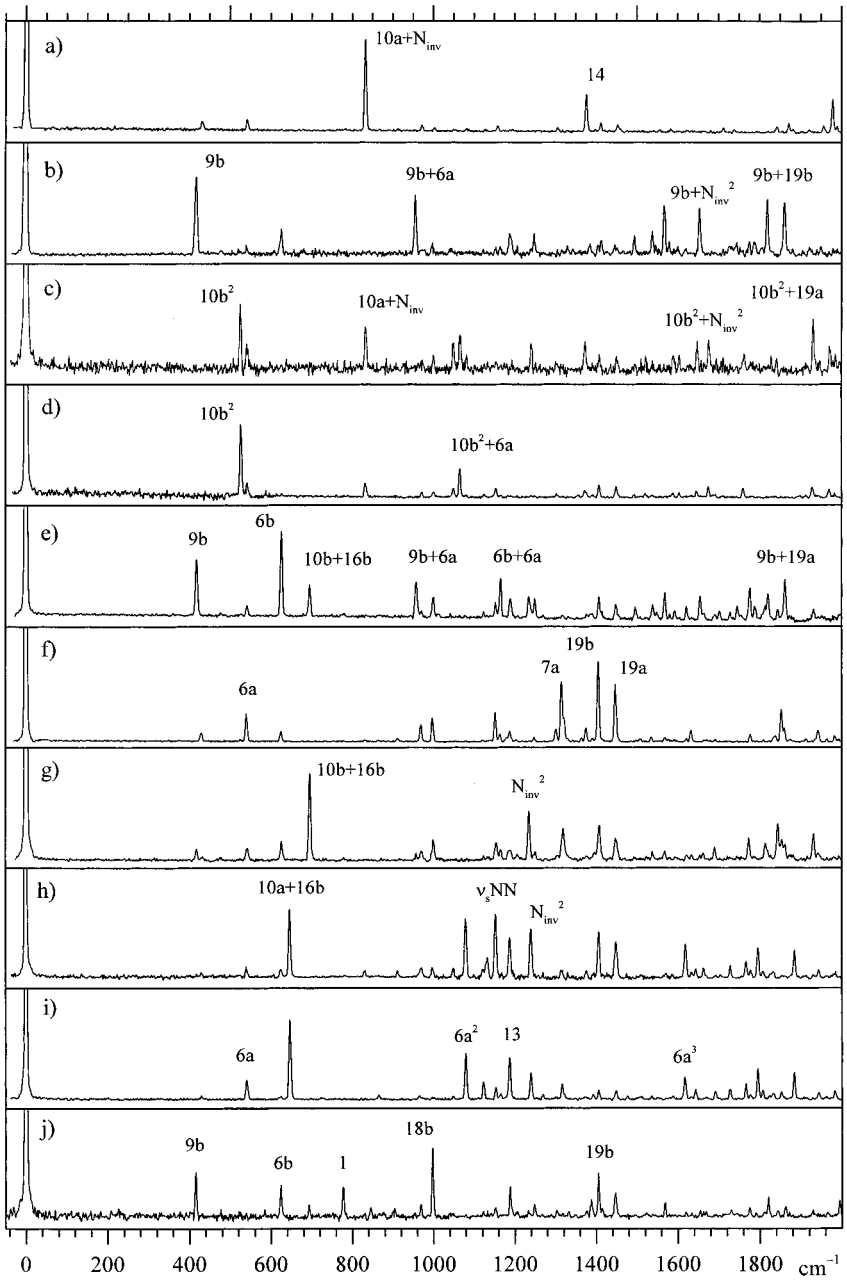

Figure 7. SVLF spectra obtained by dispersing the fluorescence from the vibronic band of 2*H*-BT at 238.7 cm^{-1} (a), 328.5 cm^{-1} (b), 330.7 cm^{-1} (c), 338.2 cm^{-1} (d), 439.2 cm^{-1} (e), 480.7 cm^{-1} (f), 481.9 cm^{-1} (g), 509.5 cm^{-1} (h), 519.9 cm^{-1} (i), and 795.6 cm^{-1} (j).

as a linear combination of an NN asymmetric stretch with an NH in-plane bending vibration δ NH. A transition at 1449 (1446) cm^{-1} can be observed in every SLVF spectrum and is assigned to the mode 19a. Frequency and deuteration shift are again in good agreement with the calculations.

The modes 8a at 1537 (1534) cm^{-1} and 8b at 1569 (1568) cm^{-1} are only weakly observed upon excitation of 0,0, but are found in almost every SVLF spectrum. In the region around 3100 cm^{-1} four CH stretching vibrations are expected (2, 7b, 20a, 20b). Due to a multitude of overtones and combination bands, the spectrum is very crowded, so that we cannot give a reliable assignment of transitions to these vibrations. The NH stretching vibration is observed at 3486 cm^{-1}, in very good agreement with an FTIR measurement of this band;[29] the N-deuterated counterpart is found at 2598 cm^{-1}.

B. Electronically Excited States. The vibrational assignment for the electronically excited state(s) is not as straightforward as in the electronic ground state. The band contour analysis shows that besides the expected *b*-type transitions, which represent the allowed a_1 modes, a great number of *a*-type bands can be observed. From symmetry consideration it follows that these bands are due to b_2 modes of 2*H*-BT. Their large intensities and number cannot solely be explained by vibrationally induced rotation of the transition dipole moment (TDM) with respect to the inertial axes, because the projection of the *a*-axis onto the TDM would still be small. Herzberg−Teller intensity stealing from a nearby electronic state with A_1 symmetry can account for these large intensities. The long (*a*) axis polarized ^1L_b of 2*H*-BT has the required A_1 symmetry. Nevertheless, this cannot be the only explanation for the great number of *a*-type transitions, which exceeds the number of available normal modes by far. Some of these intense *a*-type transitions may also be a_1 modes of the S_2 state. As long as the vibrationless origin $S_2 \leftarrow S_0$ is not determined, any vibronic analysis of the S_1 state must therefore remain provisional.

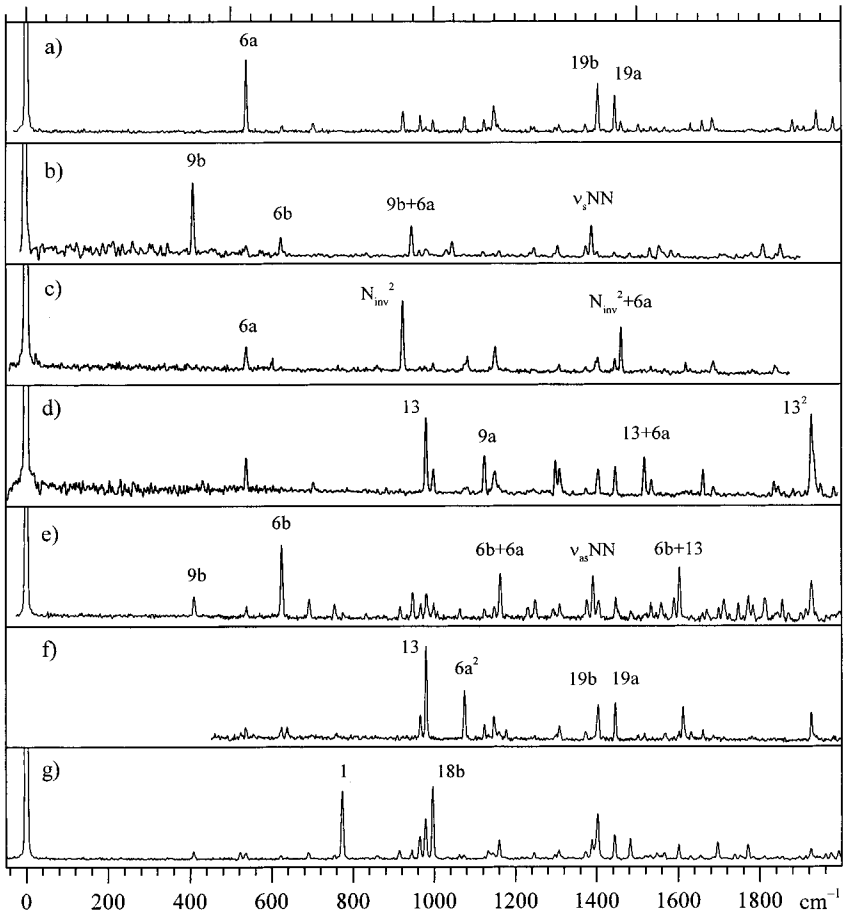

Figure 8. SVLF spectra obtained by dispersing the fluorescence from the vibronic band of 2*D*-BT at 297.9 cm^{-1} (a), 319.0 cm^{-1} (b), 352.3 cm^{-1} (c), 372.1 cm^{-1} (d), 438.4 cm^{-1} (e), 510.1 cm^{-1} (f), and 912.9 cm^{-1} (g).

Although *b*-type bands arise from totally symmetric a_1 vibrational modes *and* from overtones of nontotally symmetric vibrations, the number of *b*-type bands in the range below 500 cm^{-1} is too large compared to the calculations.

The fact that the shifted bands must have the same rotational band contour helps to get an unambiguous assignment of 2*D*- to 2*H*-BT transitions for nearly all vibronic bands. Figure 9 shows the calculated spectra of 2*H*- and 2*D*-BT in the range 200−550 cm^{-1} using frequencies and intensities from the LIF spectra. Related bands are connected by straight lines. We have simulated this spectrum for two reasons: The R2PI intensities of the two tautomers are so different that an assignment is hardly possible. On the other hand, the LIF spectrum of 2*D*-BT is disturbed by bands of the undeuterated species, due to incomplete deuteration. In our simulation the *a*-type and *b*-type bands are shown in different traces to clarify the assignment of 2*H*- to 2*D*-BT bands.

The lowest frequency band in the 2*H*-BT spectrum is observed at 238.7 cm^{-1} and shows a *b*-type rotational contour. Thus, this band must be either an a_1 fundamental or an overtone of a b_2 mode or of an out-of-plane vibration. The lowest calculated frequency in the S_0 state is 216 cm^{-1} for the 10a mode. We tentatively assign the 238.7 cm^{-1} band to the overtone of this vibration, assuming a large frequency shift and/or anharmonicity upon electronic excitation. A harmonic value of 120 cm^{-1} seems to be very low, although the corresponding harmonic frequency in indole[30,31] is comparably low at 158 cm^{-1}. The following *b*-type band is observed at 330.7 cm^{-1} and can be assigned to the overtone of 10b.

The *a*-type band at 328.5 cm^{-1} must be a fundamental b_2 mode or a combination band with b_2 symmetry. A combination of 10a (b_1) and 10b (a_2) would have the appropriate symmetry but is too far from the harmonic frequencies of the 10a (120 cm^{-1}) and 10b (165 cm^{-1}) vibration. Therefore we favor the assignment of this band to the b_2 fundamental 9b. A strong indication of the correctness of this assignment is the occurrence of 9b combination bands in the DF spectra, when exciting this band.

Most of the vibrations below 500 cm^{-1} do not shift considerably upon deuteration, with one distinct exception: the band at 480.7 cm^{-1} in 2*H*-BT is shifted to 352.3 cm^{-1}.

Around 500 cm^{-1} a deuteration shift of more than 15% is only expected for N_{inv} and the γ NH vibration, although these b_1 out-of-plane vibrations should be forbidden. They show extremely different displacement vectors for 2*H*- and 2*D*-BT as described in section III. Therefore we assign the band at 480.7 (352.3) cm^{-1} to the first overtone of one of these vibrations. It is true that this value is far from the (harmonic) calculations for the S_0, but these large amplitude motions may well have a quite anharmonic potential in the S_1 state and, moreover, a different potential compared to the S_0 state. This large deuteration shift of the vibrational frequency may also account for the large blue shift of the electronic origin.

The totally symmetric 6a vibration is assigned to the *b*-type band at 509.5 cm^{-1}, while mode 6b is assigned to the *a*-type band at 631.9 cm^{-1}. All vibronic frequencies discussed up to now are considerably lower than the calculated ground-state vibrational frequencies. For vibrations above 600 cm^{-1} this poor agreement between experimental frequencies and (ground-state) calculations excludes further assignments at the moment. Presently we are performing calculations on the electronically excited states in order to get a deeper insight into the vibronic

TABLE 4: Relative Frequencies and Intensities Obtained from the SVLF Spectra of 2*H*-BT[a]

		excited vibronic band										
rel freq	assignment	0_0^0	239 (a)	329 (b)	331 (c)	338 (d)	439 (e)	481 (f)	482 (g)	510 (h)	520 (i)	796 (j)
417	9b			100			70		15			67
430	$10a^2$		13					12	7	11	6	
526	$10b^2$				100	100		4		7		10
542	6a	91	15	17	45	22	20	37	16	20	26	
626	6b			36		7	100	14	24	15	5	50
648	10a+16b									100	100	
695	10b+16b						42		100			23
778	1						3		5	7		47
833	$10a+N_{inv}$		100		67	21		4		14		
866	12							3			7	
957	9b+6a			78			45		10			6
971	15	21	9	11		9	13	22	13	18	6	23
1000	18b	27	6	19	30	9	28	31	26	18	3	100
1050	$10b^4$				47	14				17	5	
1067	$10b^2+6a$			13	58	40						
1081	$6a^2$	27	5		31	5				86	58	
1124	9a	43				6	12	3		16	23	
1133	18a	22								32		
1154	ν_s NN	95		14		14	23	37	22	93	16	19
1165	6a+6b	21	8	15			49	11	14	11	8	
1189	13	17		31			27	14	13	60	53	47
1239	N_{inv}^2	100		16	47		29		58	72	34	
1250	3			31			27	7	12			23
1304	ν_{as} NN		6		21	7	9	17	7			15
1316	7a							75		14	21	
1321	6a+1							31	38			
1332		10		16								13
1375	14	25	42		49	11	10	18		14		14
1388		12		18								29
1395	$10b^2+16b^2$					5			15		8	
1407	19b	84	11	16	31	18	29	100	42	68	12	66
1414	ν_{as} NN+δ NH			22			13					17
1449	19a	86	9	17	28	17	20	72	27	54	12	39
1495	$6a^2+9b$			28		5	17		6			
1523	$10b^2+18b$				29	7			6			5
1537	8a	23		33	23	5	20	7	12		5	
1549				17			12					
1569	8b	13		65			33	6	13	10		25
1591	$10b^4+6a$				30	8	13				5	
1604	$10b^2+6a^2$			15	31	8						
1619	$6a^3$	13		12			18	5	8	51	29	6
1633		18						15	8	11		
1646	$10b^2+9a$				50	10				16	14	
1657	N_{inv}^2+9b	31		62			29		8			9
1665	$N_{inv}^2+10a^2$	17					11	3	11	17		8
1677	$10b^2+\nu_s$ NN				52	16						
1691	$6a+\nu_s$ NN	56					9	4	17	6	11	
1729	$10a+16b+6a^2$						12			20	13	9
1747	6b+9a			19			18					
1762	$N_{inv}^2+10b^2$				32	14						
1767	10a+16b+9a									26	21	
1776	$N_{inv}^2+6a/6b+\nu_s$ NN	54		21			38	10	28	14	6	13
1790	$9b+14/6a+6b^2$			20			18					6
1796	$6a+6b^2/10a+16b+\nu_s$NN									45	39	
1815	6b+13/10b+16b+9a						19		22			7
1820	9b+19b			73			32					33
1844			7		26		15		44			11
1854	$17b^2$							41	25		10	
1862	9b+19a			68			48	18	20			20
1885	$10a+16b+N_{inv}^2$								8	42	34	
1930	$10b^2+19b$	51			80	15	15		32			15
1944	6a+19b							15	10	14	9	
1971	$10b^2+19a$				43	12						
1982	6a+19a	43	37		23	7		8		12	12	

[a] Column heads give the frequency of the excitation band relative to the electronic origin (letters refer to Figure 7), while the first column presents the frequency of the SVLF band relative to the excitation frequency. The intensity for each spectrum is scaled to the most intense band with the excitation wavelength excluded.

structure of BT in different electronic states. Especially coupling to the S_2 state may account for the very congested spectrum above 1000 cm^{-1}.

If one compares the intensities from LIF, R2PI, and SHB spectra, there is a very poor correspondence. In the low-frequency part of the spectrum this is probably due to the fact

TABLE 5: Relative Frequencies and Intensities Obtained from the SVLF Spectra of 2*D*-BT[a]

		excited vibronic band							
rel freq	assignment	0_0^0	298 (a)	319 (b)	352 (c)	372 (d)	438 (e)	510 (f)	913 (g)
409	9b			100			34		14
526	$10b^2$							14	12
538	6a	85	100	18	41	48	22	19	11
624	6b	13	11	29			100	19	8
692	10b+16b						30		12
704			14			20			
755							24		8
777	1						14		95
860	12				15				7
916							21		15
924	N_{inv}^2	12	30		100				
947	9b+6a			44			38		15
966	15	40	25	12			25	31	33
981	13	100	10	14		97	37	100	57
999	18b		19		19	37	26		100
1033	9b+6b (?)	9		13					6
1064	$10b^2$+6a						18		9
1075	$6a^2$	21	24		16	14		56	9
1083					27	15			
1124	9a	34	19	10		50	18	22	
1133	18a								14
1138	18a				13				
1148	ν_s NN	36	38		1	29	21	30	11
1153			1		39	32			
1159		14	12						
1161	6a+6b			11			63	14	28
1231							20		
1248	$3/6b^2$		9	15		12	29	11	11
1296	δ NH						18		9
1301	$16a^2$	20	7			47		11	
1309	7a	14	10	18	17	36	24	19	14
1374	14	14	12	17	15	13	29	14	12
1390	ν_{as} NN			44			60		29
1404	19b	45	56	10	26	30	28	41	63
1446	19a	44	46	9	23	37	33	43	35
1462	N_{inv}^2+6a		14		70				
1484				8			15		31
1503	11^2 (?)	15	13					11	
1519	13+6a	49				47		12	7
1534	8a		9	15	13	22	26		8
1557				18			26		
1568	8b	7	9		10			12	11
1591	6b+15						32		
1603	6b+13						71	22	22
1632		9	14		10	11		14	7
1662	6a+9a	14	17			34	13	16	
1686	6a+ν_s NN	18	22		1	14			
1698	$6a^2$+6b		1				19		25
1713							30		
1750	6b+9a						25		7
1773	6b+ν_s NN						34		22
1783	6a+$6b^2$			9	9		22		6
1811	9b+19b			20			31		7
1838	N_{inv}^4				15	21			
1845	6a+7a				12	15	13		
1854	9b+19a/$17b^2$			19			29		6
1881			18		60[b]	13			
1910		7	10				17		6
1926	13^2	30				100	53	33	16
1933						50			
1939	6a+19b	19	32						
1950	13+15					20			
1980	6a+19a	20	23			15		9	

[a] Column heads give the frequency of the excitation band relative to the electronic origin (letters refer to Figure 8), while the first column presents the frequency of the SVLF band relative to the excitation frequency. The intensity for each spectrum is scaled to the most intense band with the excitation wavelength excluded. [b] Not shown in spectrum 7c.

that the second photon excites only little above the IP. Between 500 and 900 cm^{-1} the LIF and R2PI intensities are quite similar, but above 900 cm^{-1} they differ again dramatically. The most intense bands in the SHB spectra are in this region. This can be explained under the assumption that the second electronic state shows only weak fluorescence, but can be ionized with a similar cross section as the S_1 state. This would lead to an enhancement of the hole-burning efficiency. The origin of this

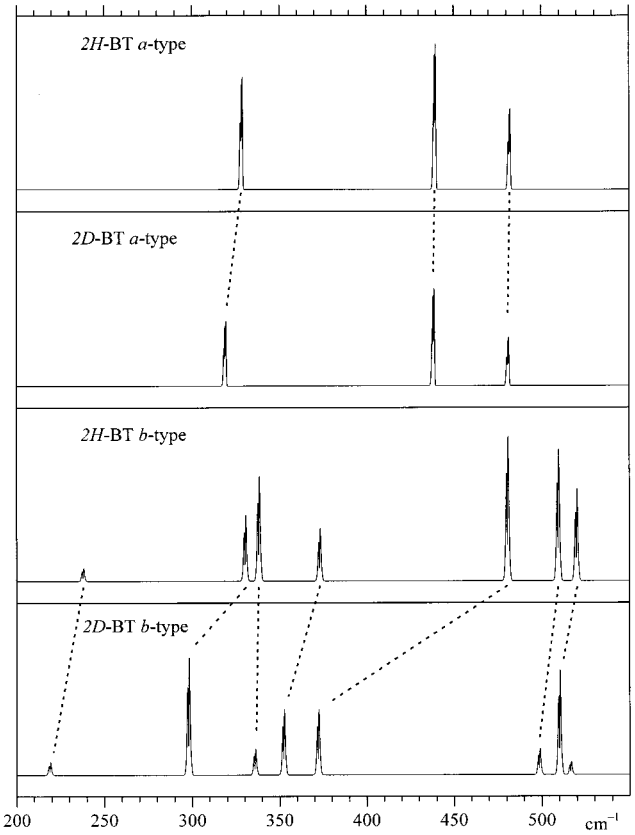

Figure 9. Calculated LIF spectrum of 2*H*- and 2*D*-BT between 200 and 550 cm^{-1} above the electronic origin deconvoluted into *a*- and *b*-type bands. The band positions and relative intensities have been taken from the experimental LIF spectrum; the rotational contours, from the simulations described in section IV.C.

second electronically excited state would then be located somewhere around 900 cm^{-1} above the $S_1 \leftarrow S_0$ origin.

VI. Conclusions

Starting from the well-defined electronic origin of the 2*H*-BT, vibrational levels have been determined in the ground and first excited state(s). Absorption due to the second possible tautomer was ruled out using double-resonance spectroscopy techniques such as SHB and DF.

As already known from previous LIF measurements,[21] the electronic spectrum shows a large number of vibronic transitions. Using LIF with higher resolution we were able to differentiate these states into *a*- and *b*-type transitions. The large intensities of the b_2 vibronic levels can be made possible via Herzberg−Teller coupling with a nearby S_2 state of A_1 symmetry.

The large number of vibronic levels and a possible mixing of states prevent a clear assignment of the observed transitions in the S_1 and S_2 state. The close vicinity of both states even queries the picture of vibronic eigenfunctions which can be labeled according to one of these states. Nevertheless we were able to assign nearly all a_1 and b_2 modes in the electronic ground state by comparison of SVLF spectra with the results of an ab initio normal-mode analysis. The nearly exclusive appearance of a_1 and b_2 modes upon excitation of 0,0 indicates planarity in the S_0 and the S_1 state in agreement with C_{2v} selection rules. In contrast to FTIR or Raman spectra of benzotriazole this technique is selective for the 2*H*-tautomer via the resonant excitation process.

Acknowledgment. This work is part of the dissertation of W.R. The authors are grateful to Prof. Karl Kleinermanns and Prof. Wolfgang Domcke for helpful discussions. The ab initio calculations were performed at the Regionales Rechenzentrum Köln and at the Universitätsrechenzentrum Düsseldorf. We gratefully acknowledge the financial support of the Deutsche Forschungsgemeinschaft.

References and Notes

(1) Cotton, J. B.; I. R. Scholes *Br. Corros. J.* **1967**, *2*, 1.
(2) Maquestiau, A. van Haverbeke, Y.; Flammang, R.; Pardo, M. C.; Elguero, J. *Org. Mass Spectrom.* **1973**, *7*, 1267.
(3) Catalán, J.; Pérez, P.; Elguero, J. *J. Org. Chem.* **1993**, *58*, 5276.
(4) Escande, P. A.; Galigné, J.; Lapasset, J. *Acta Crystallogr. B* **1974**, *30*, 1490.
(5) Palmer, M. H.; Kurshid, M. M. P.; Rayner, T. J.; Smith, J. A. S. *Chem. Phys.* **1994**, *182*, 27.
(6) Velino, B.; Cané, E.; Gagliardi, L.; Trombetti, A.; Caminati, W. *J. Mol. Spectrosc.* **1993**, *161*, 135.
(7) Melandri, S.; Caminati, W.; Favero, L. B.; Millemaggi, A.; Favero, P. G.; *J. Mol. Struct.* **1995**, *252*, 253.
(8) Katritzky, A. R.; Yannakopoulou, K.; Anders, E.; Stevens, J.; Szafran, M.; *J. Org. Chem.* **1990**, *55*, 5883.
(9) Tomás, F.; Abboud, J.-L.; Laynez, J.; Notario, R.; Santos, L.; Nilsson, S. O.; Catalán, J.; Claramunt, R. M.; Elguero, J. *J. Am. Chem. Soc.* **1989**, *111*, 7348.
(10) Tomás, F.; Catalán, J.; Pérez, P.; J. Elguero, *J. Org. Chem.* **1994**, *59*, 2799.
(11) Negri, F.; Caminati, W. *Chem. Phys. Lett.* **1996**, *260*, 119.
(12) Fischer, G.; Cao, X.; Purchase, R. L. *Chem. Phys. Lett.* **1996**, *262*, 689.
(13) Hitherto unpublished results.
(14) O'Sullivan, D. G. *J. Chem. Soc.* **1960**, 3653.
(15) Mohan, S.; Settu, K. *Ind. J. Pure Appl. Phys.* **1993**, *31*, 850.
(16) Konopski, L.; Kielczewska, A.; Maslosz, J. *Spectrosc. Lett.* **1996**, *29*, 143.
(17) Bigotto, A.; Pandey, A. N.; Zerbo, C. *Spectrosc. Lett.* **1996**, *29*, 511.
(18) Schütt, H.-U.; Zimmermann, H. *Ber. Bunsen-Ges. Phys. Chem.* **1963**, *67*, 54.
(19) Platt, J. R. *J. Chem. Phys.* **1949**, *17*, 484.
(20) Specker, H.; Gawrosch, H. *Chem. Ber.* **1942**, *75*, 1338.
(21) Jalviste, E.; Treshalov, A. *Chem. Phys.* **1993**, *172*, 325.
(22) Cané, E.; Trombetti, A.; Velino, B. *J. Mol. Spectrosc.* **1993**, *158*, 399.
(23) Berden, G.; Jalviste, E.; Meerts, W. L. *Chem. Phys. Lett.* **1994**, *226*, 305.
(24) Gerstenkorn, S.; Luc, P. *Atlas du spectre d'absorption de la molecule d'Iode*; CNRS: Paris, 1978.
(25) Frisch, M. J.; Trucks, G. W.; Schlegel, H. B.; Gill, P. M. W.; Johnson, B. G.; Robb, M. A.; Cheeseman, J. R.; Keith, T.; Petersson, G. A.; Montgomery, J. A.; Raghavachari, K.; Al-Laham, M. A.; Zakrzewski, V. G.; Ortiz, J. V.; Foresman, J. B.; Peng, C. Y.; Ayala, P. Y.; Chen, W.; Wong, M. W.; Andres, J. L.; Replogle, E. S.; Gomperts, R.; Martin, R. L.; Fox, D. J.; Binkley, J. S.; Defrees, D. J.; Baker, J.; Stewart, J. P.; Head-Gordon, M.; Gonzalez, C.; Pople, J. A. Gaussian 94; Gaussian, Inc.: Pittsburgh, PA, 1995.
(26) Varsanyi, G. *Assignments for Vibrational Spectra of 700 Benzene Derivatives*; Wiley: New York, 1974.
(27) Bickel, G. A.; Demmer, D. R.; Outhouse, E. A.; Wallace, S. C. *J. Chem. Phys.* **1989**, *91*, 6013.
(28) Jacoby, Ch.; Spangenberg, D.; Janzen, Ch.; Schmitt, M. In preparation.
(29) Roth, W.; Westphal, A.; Janzen, Ch.; Schmitt, M. In preparation.
(30) Barstis, T. L. O.; Grace, L. I.; Dunn, T. M.; Lubman, D. M. *J. Phys. Chem.* **1993**, *97*, 5820.
(31) Bickel, A.; Remmer, D. R.; Allison, E. A.; Wallace, S. C. *J. Chem. Phys.* **1989**, *91*, 6013.